

Magazine of Civil Engineering

ISSN 2712-8172

journal homepage: http://engstroy.spbstu.ru/

Research article **UDC 624**

DOI: 10.34910/MCE.132.7



Stability of gypseous soils slopes stabilized with cutback asphalt and lime using the finite element method

Z. Abd Hacheem¹, S. Al-Khyat², K.A. Saeed², S.H.L. Fartosy² D



Mustansiriyah University, Baghdad, Iraq

☑ dr.sabah77@uomustansiriyah.edu.iq

Keywords: factor of safety, slope stability, binders, bituminous soil stabilization, ADONIS.

Abstract. Gypseous soils are widely distributed all over the world, particularly in Iraq. These soils exhibit unpredictable behaviour including losing strength and collapsing upon wetting. Treatment of gypseous soil is necessary to improve its geotechnical properties and assess its potential applications in engineering practices. Compacted gypseous soil samples stabilized with different binders, including cutback asphalt and lime. Slope stability analysis was performed to determine the factor of safety and analyze the behaviour of the stabilized gypseous soil. ADONIS 3.25, a computer program based on the finite element method, was used to characterize the gypseous soil and to analyze the slope stability by Mohr-Coulomb failure criteria and visco-plastic algorithm. The effects of varying the percentages of binders and the slope angle (H:V) were investigated. A total of thirty numerical analyses were performed. Results of the numerical analysis indicated that the best slope stability was obtained when the gypseous soils stabilized with 4 %cutback asphalt and 3 % lime at a slope angle of 3H:1V. It was also observed that the slope angle has a considerable effect on the safety factor of the slope, such that, the steepest the slope angle - the lowest the safety factor.

Acknowledgment: The authors would like to appreciate the great support they received from Mustansiriyah-University (https://www.uomustansiriyah.edu.iq), Baghdad- Iraq which was helpful to achieve this research.

Citation: Abd Hacheem, Z., Al-Khyat, S., Saeed, K.A., Fartosy, S.H.L. Stability of gypseous soils slopes stabilized with cutback asphalt and lime using the finite element method. Magazine of Civil Engineering. 2024. 17(8). Article no. 13207. DOI: 10.34910/MCE.132.7

1. Introduction

Slope stability analysis is required in geotechnical projects, such as cuts, fills, dams, and road embankments, since it concerns the safety of human life and property. As a result, appropriate slope inspections, remedies, and engineering solutions must be provided to prevent potentially devastating collapse [1]. A slope failure is the failure of a mass of soil in a downward and outward movement of a slope. The surface along which the slide occurs has different shapes and represents the surface of minimum resistance. A variety of methods and techniques have been used for the analysis of earth slopes, including the finite element method (FEM) based on cohesion (c) and internal friction angle (Φ) reduction, the finite difference method (FDM), the limit analysis (LA), and a combination of the FEM and the FDM [2]. Slope geometry, soil type, soil shear strength, soil stratification, groundwater condition, and seepage significantly impact slope failure and should be considered during slope stability analysis [3].

Slope stabilization can be accomplished using a variety of approaches including structural and geometric methods [4]. For example, reducing the slope height (H) results in a higher factor of safety (FS) of the slope. Many other studies have employed soil improvement and stabilization to investigate the

© Abd Hacheem, Z., Al-Khyat, S., Saeed, K.A., Fartosy, S.H.L., 2024. Published by Peter the Great St. Petersburg Polytechnic University

behaviour of reinforced slope stability soils made of various materials [5–8]. Soil stabilization alters the engineering properties of soils, such as gypseous soils, in such a way that it gains long-term strength and stability. Gypseous soils are soils that contain gypsum and are susceptible to losing strength when introduced to wetting. Gypseous soils with varied proportions of gypsum contents cover a large portion of Iraq. The estimated coverage area of gypseous soils was reported to be about 12.2 % by Barazanji [9] as shown in Fig. 1. The amount of gypsum in the upper north and centre parts of the Euphrates and Tigris beds can reach 80 %, whereas the gypsum content of the Al-Jazirah area ranges from 3 % to 10 % in the upper parts to 50 % in the lower parts [10].

Several stabilizers can be used to improve the characteristics of gypseous soils by limiting the effect of water, such as cutback asphalt and lime. Bituminous soil stabilization is one of the oldest methods for improving soil properties. Cutback asphalt dissolves in certain solvents, such as gasoline, to improve its fluidity and workability. Cutback asphalt is classified into rapid, medium and slow curing cutback depending on the solvent used [11]. When the solvent evaporates, the bitumen remains to bond the particles together. The asphalt acts as a waterproofing agent and enriches the cohesive strength and durability characteristics of gypseous soils. Asphalt coating the soil particles provides a membrane that prevents or limits water infiltration, which would otherwise result in a loss of soil strength. In the waterproofing of bituminous materials, two hypotheses can be explained. The theory of the plug at which the bituminous globules operate as plugs or stoppers in the soil void spaces or soil capillaries, removing or eliminating the flow pathways via which surface water might enter or exit the mix [12]. The membrane theory is the second theory that assumes a thin bituminous film will operate as a covering or segregator for individual soil particles, resulting in the same consequence of waterproofing the soil as the plug theory, however in a slightly different way. Cutback asphalt also acts as a cementing agent, such that the soil particles also adhere to the asphalt allowing it to act as a binder or cementing agent. The cementing effect thus increases shear strength by increasing cohesion [13]. According to the intimate mix theory, the efficiency of a bituminous material's cementing activity is primarily explained by the adhesion that occurs between the binder and soil particles. The action of surface tension, adsorption, and other features of the solid and liquid surfaces interact to produce this adhesion. Since water has a higher wetting power than any bituminous binder, full cementation and total adhesion can only be achieved when the binder displaces any water on the surface and when too much binder is applied and the film covering around the particles becomes too thick. Because the bituminous cohesiveness is reduced, contact between the particles is prevented, and strength is reduced. Lime soil stabilization, on the other hand, has been often used. The lime is added in the form of calcium oxide or calcium hydroxide to the soil at the optimum moisture content [14].

Generally, all fine-grained soils treated with lime show lower plasticity, enhanced workability, and reduced volume change characteristics. Not all soils, however, have better strength properties. The characteristics of a soil-lime mixture are influenced by several factors, the most important of which are soil type, lime type, lime percentage, and curing conditions [15]. When lime is added to fine-grained soil, it causes a series of reactions. Cation exchange is taken place in which the positively altered ions cling to the surface of clay particles. The common cation replacement happens in the form of lyotropic series (Na+ K+ Mg++ Ca++). It is clear from this series that if multivalent cations are accessible in the soil, monovalent cations will be replaced by them [16]. As a result of the modifying effects of electrolytes on the extension of the electrical double layer from the surfaces of clay particles, clays flocculate when electrolytes are added. The electrolyte reduces the electrostatic repulsive interactions between clay particles by repressing the double layer. This causes a net pull between negatively charged faces and positively charged edges of neighboring clay particles, especially between negatively charged faces and positively charged edges of nearby clay particles [17]. The other series of reactions can occur in the form of pozzolanic reactions. The pozzolanic reactions are lime reactions with soil silica and/or alumina that result in the development of a stiff water-insoluble gel that cements the soil particles [18]. When lime reacts with the silica and/or alumina, it forms calcium silicate hydrated and/or calcium aluminate hydrated in the form of a soluble gel that coats and cements soil particles as it hardens. Pozzolanic reactions are lime-dependent, and strength improved slowly and steadily over time [17]. A potentially negative impact reaction on the stabilizing process could be lime reacts with carbon dioxide in the air to generate calcium carbonate, a rather weak cementing agent (CaCO3) [15].

Stabilization of gypseous soil with asphalt and lime has been recognized as an economical treatment in Iraq due to the abundance of limestone from which lime is manufactured and the availability of cutback asphalt as refineries wastes [19]. These stabilizers have been successfully used to improve the engineering properties of gypseous soils. Studies on examining the potential application of stabilized gypseous soils in engineering practice, such as earth slopes are scarce. Therefore, this study aims to evaluate the slope stability of gypseous soils stabilized with different percentages of cutback asphalt and lime using the FEM.

2. Materials and Methods

Experimental results of a study conducted by Al-Safarani [19] was used in this study. Al-Safarani [19] used a gypsum-rich soil that obtained from Abu Ghraib, 30 km from Baghdad with 48.6 % gypsum content. The sample was collected at a depth of 0.5–1.0 m below the natural ground level [19]. Table 1 lists the physical and chemical characteristics of the soil used [19]. Soil stabilization was achieved using the hydrated lime (Ca(OH)₂) generated when quick lime reacts chemically with water. Table 2 shows the chemical composition of the lime used [19]. A medium cutback asphalt [MC-30] produced by the Dora refinery in Baghdad was used. The properties of asphalt used are given in Table 3 [19].

Two groups of stabilized samples were prepared. The first group were stabilized with 0 %, 2 %, 4 %, 6 %, 8 %, and 10 % cutback asphalt (MC). While, lime (L) of 3 %, 5 %, 7 %, and 9 % were added to the soil samples with the best percentage of cutback asphalt to stabilize the second group. It was found that the best percentage of cut back asphalt was 4 % as it shows better soil behavior in terms of compression, permeability, collapse, and compaction. The stabilized samples were air-cured for seven days and then soaked for about one hour. A series of direct shear tests were conducted on the prepared samples and the results are summarized in Table 4 [19]. The dry unit weight for each condition was obtained from the compaction tests.

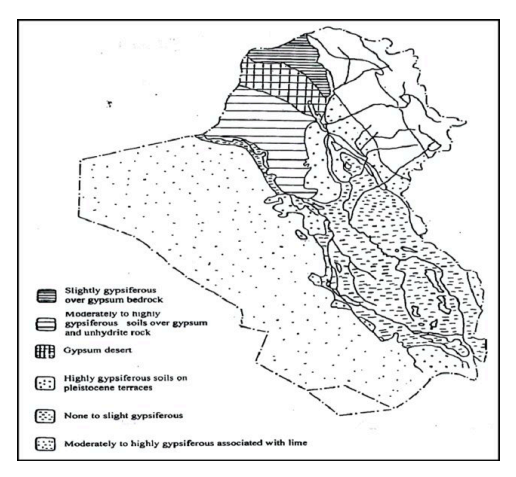


Figure 1. Gypseous soil in Iraq (after, Barazanji [9]).

Table 1. Geotechnical properties of the soil [19].

Soil property	Standard	Result
Gypsum content (%)		48.6
Liquid limit (%)	BS1377: 1975, test No.2, A	31.0
Plastic limit (%)	BS 1377:1975, test No.3	NP
Specific gravity of soil solids	BS 1377:1975, test No.6 B	2.39
Maximum dry unit weight (kN/m³)	ASTM D698-78	16.0
Optimum moisture content (%)		14.7
Sand (%)	ASTM D422-72	90.5
Fines (%)	ASTM D422-72	9.5
Soil classification	USCS	SP-SM
Sulphate content (SO ₃) (%)	BS 1377:1975, test No.5	22.21
Total soluble salt (T.S.S) (%)	BS 1377:1975, test No.8	63.7
Chloride content (CL) (%)	BS 1377:1975, test No.7	0.09
Organic matters (%)	BS 1377:1975, test No.3	0.2
рН	BS 1377:1975, test No.9	8.1

Table 2. Chemical analysis of Lime [19].

Composition	Percentage by weight
CaO	72.33
MgO	6.83
SiO ₂	10.25
Al_2O_3	1.68
Fe ₂ O ₃	8.13

Table 3. Properties of the cutback asphalt after Dora Refinery lab. Baghdad [19].

Property	MC-30	
Kinematics viscosity at 60°C (c.Stoke)	75–150	
Specific gravity of soil solids	0.99	
Distillate, %vol. of the total, Distillate to 360°C		
To 225°C	25 max.	
To 260°C	40-70	
To 315°C	75–93	
Residue from distillation to 360°C%vol. by difference	50 min.	
Test on residue from the distillation	120–300	
Penetration at 25°C (100g, 5 sec.)	120–300 100 min.	
Ductility at 25°C	99.5 min.	
Solubility in CCl4, %wt. min.	33.J IIIII.	

Table 4. The effect of binder on shear strength parameters [19].

Percentage of binder	c (kPa)	Ø (degree)	γd (kN/m³)
0 % MC	10.0	46.3	16.00
2 % MC	28.0	39.8	15.25
4 %MC	39.5	42.0	14.90
6 % MC	43.5	37.6	14.75
8 % MC	38.5	37.0	14.60
10 % MC	37.0	36.2	14.20
4 % MC + 3 % L	51.5	44.5	14.90
4 % MC + 5 % L	53.0	40.2	14.85
4 % MC + 7 % L	36.1	39.8	14.70
4 % MC + 9 % L	35.0	28.6	14.70

2.1. Failure Criteria

Several failure criteria for characterizing the strength of soil as an engineering material have been developed. The best-known criterion for soils with both frictional and cohesive components of shear strength is Mohr–Coulomb, which has the shape of an irregular hexagonal cone in primary stress space. Cylindrical failure criteria are acceptable for metals or undrained clays that behave in a frictionless manner ($\phi u \approx 0$, ϕu is the angle of internal friction in undrained condition). These are the most basic conditions, and they are not affected by the initial invariant S or σ_m . Since the Tresca criterion is a particular case of the Mohr–Coulomb criterion, it does not require independent mathematical treatment [20]. According to the Mohr–Coulomb criterion, the shear strength increases with increasing normal stress on the failure plan [21].

$$\tau = C + \sigma \tan \varphi, \tag{1}$$

where τ is the shear stress on the failure plane, C is the cohesion of the material, σ is the normal effective stress on the failure surface, and ϕ is the angle of internal friction. This failure criterion is shown graphically in Fig. 2. The concept of the Mohr circle can be used to express the criterion in terms of principal stresses.

According to Fig. 2,

$$\frac{\sigma_1 - \sigma_3}{2} = AB + BF. \tag{2a}$$

That is

$$\frac{\sigma_1 - \sigma_3}{2} = OA \sin \varnothing + C \cos \varnothing. \tag{2b}$$

Hence:

$$\frac{\sigma_1 - \sigma_3}{2} = \frac{\sigma_1 + \sigma_3}{2} \sin \varnothing + C \cos \varnothing. \tag{2c}$$

Here, σ_1 & σ_3 are the major and minor principal stresses, respectively. In the stress space, Equation (2c) describes an uneven hexagonal pyramid. The projection of this surface on the π -plane is shown in Fig. 2. The three stress invariants are σ_m , t and θ . In which σ_m describes the mean stress, t describes the shear stress, and θ gives the direction of the shear stress. The relationship between principal stresses and invariants is given as follows.

$$\sigma_1 = \sigma_m + 2/3\,\overline{\sigma}\sin\left(\theta - \frac{2\pi}{3}\right);$$
 (3a)

$$\sigma_2 = \sigma_m + 2/3\,\overline{\sigma}\sin(\theta);\tag{3b}$$

$$\sigma_3 = \sigma_m + 2/3\,\overline{\sigma}\sin\left(\theta + \frac{2\pi}{3}\right),$$
 (3c)

where:

$$\sigma_m = S/\sqrt{3}, \ \overline{\sigma} = t\sqrt{\frac{2}{3}}, \ S = \frac{1}{\sqrt{3}}(\sigma_x + \sigma_y + \sigma_z);$$
 (4)

$$t = \frac{1}{\sqrt{3}} \left[\left(\sigma_x - \sigma_y \right)^2 + \left(\sigma_y - \sigma_z \right)^2 + \left(\sigma_z - \sigma_x \right)^2 + 6\tau_{xy}^2 + 6\tau_{yz}^2 + 6\tau_{zx}^2 \right]^{1/2}; \tag{5}$$

$$\theta = \frac{1}{3}\arcsin\left(\frac{-3\sqrt{6}J_3}{t^3}\right),\tag{6}$$

where:

$$J_3 = S_x S_y S_z - S_x \tau_{yz}^2 - S_y \tau_{xz}^2 - S_z \tau_{xy}^2 + 2\tau_{xy} \tau_{yz} \tau_{zx}. \tag{7}$$

And

$$S_x = \frac{\left(2\sigma_x - \sigma_y - \sigma_z\right)}{3},\tag{8}$$

etc.

The substation of σ_1 and σ_3 from equations (3a and 3c) in equation (2c) provides the function

$$F = \sigma_m \sin \varnothing + \overline{\sigma} \left(\frac{\cos \theta}{\sqrt{3}} - \frac{\sin \theta \sin \varnothing}{3} \right) - C \cos \varnothing. \tag{9}$$

Which is dependent upon all three invariants $(\sigma_m, \overline{\sigma}, \theta)$. The Tresca criterion is obtained from equation (3) by using $(\emptyset = 0)$.

$$F = \frac{\overline{\sigma}\cos\theta}{\sqrt{3}} - C_u. \tag{10}$$

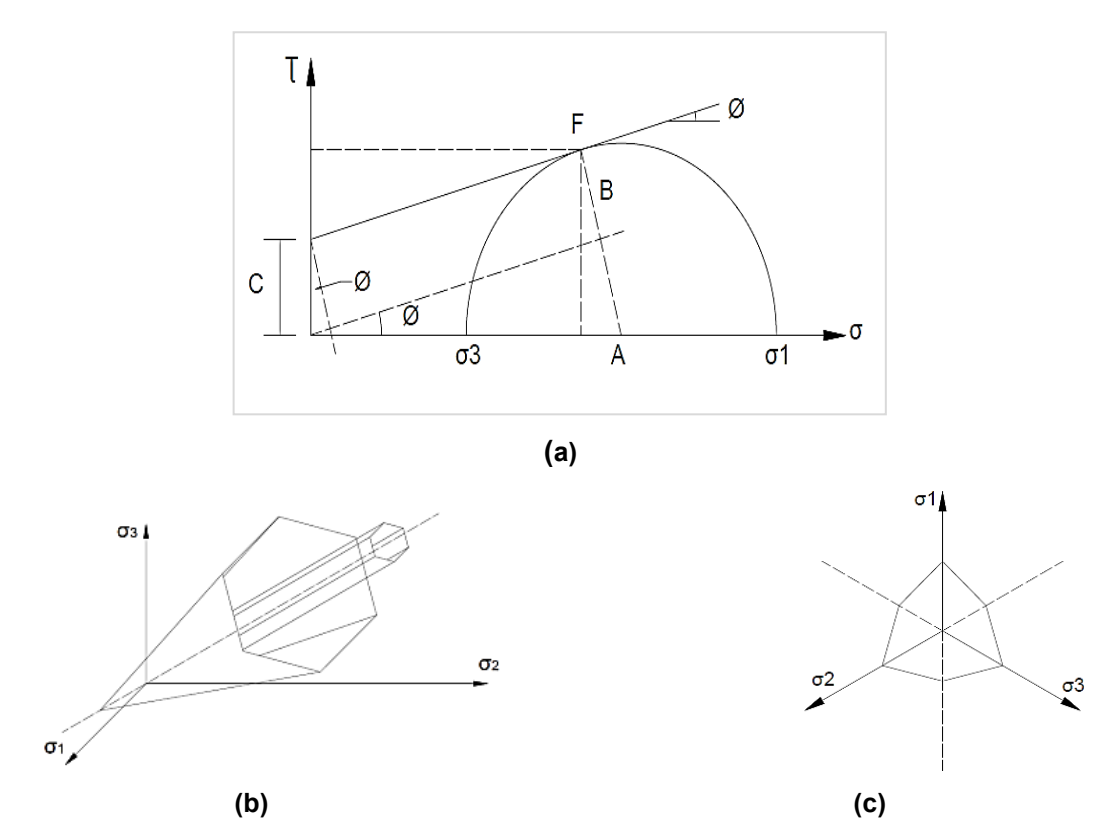


Figure 2. Mohr–Coulomb criteria on (a) σ – τ -plane, (b) stress space and (c) π plane.

2.2. Finite Element Method

The FEM is often used to obtain a realistic evaluation of stresses and deformations within earth structures as an approximate solution for gypseous soil. The results of finite element analysis can also be effectively used to evaluate the overall degree of safety and stability of these structures. The proper modelling of materials behavior and the efficient simulation of different loading conditions confirm to a high extent the reliability of the finite element results. The mathematical formulation related to the theoretical aspects of the finite element techniques is presented by Reddy [22].

The solution technique utilized in the present analysis is based on the modified Newton–Raphson method where the elastic solutions are repeated for a constant stiffness matrix. To achieve the required convergence, the load vector (the right-hand side) is to be changed iteratively. The following equations are used for each load increment:

$$K\delta^i = P^i. (11)$$

Must be solved for displacements δ^i where i represents the iteration number. The element displacement increments u_i are extracted from the nodal displacement vector oi and these lead to total strain increment according to the strain-displacement relationships:

$$\Delta \varepsilon^i = B u^i, \tag{12}$$

where B is the B-matrix of an element. If the material is yielding, the strains will comprise both elastic and plastic or visco-plastic components, as given in Equation (13):

$$\Delta \varepsilon^{i} = \left(\Delta \varepsilon^{e} + \Delta \varepsilon^{P}\right)^{i}. \tag{13}$$

Only the elastic strain increments $\Delta \varepsilon^e$ cause stresses to be generated by the elastic stress-strain matrix $\left(D^e\right)$; thus:

$$\Delta \sigma^i = D^e \left(\Delta \varepsilon^e \right)^i. \tag{14}$$

These stress increments are added to the stresses already existing from the previous load step and updated stresses are substituted into the failure criterion. If stress redistribution is required, the load increment vector P_i in equation is changed (15). This load vector, in general, holds two sorts of loads as shown by:

$$P_i = P_a + P_b^i, (15)$$

where P_a denotes the actual applied load increase, and P_b^i denotes the body load vector, which fluctuates from iteration to iteration. The P_b^i vector must be self-equilibrating in order for the system's net load to be unaffected.

The visco-plasticity algorithm established by Zienkiewicz [23] is used to generate the body-loads vector. The material is allowed to endure stresses that are outside the failure criterion for finite elements in this manner (periods). Overshoot of the failure criterion, denoted by a positive value of (f), is a crucial component of the approach and is utilized to create the algorithm. The plastic strains generated by this algorithm are referred to as visco-plastic strains because their rate is proportional to the amount by which yield has been violated by the expression:

$$\xi^{VP} = F \frac{\partial Q}{\partial \sigma},\tag{16}$$

where the potential function (Q) is used instead of the yield function to account for the non-associative flow rule.

For dimensional considerations, a pseudo-viscosity property equal to unity is implied on the right-hand side of Equation (16). The increase of visco-plastic strain is accumulated from one "time step" or iteration to the next by multiplying the visco-plastic strain rate by a pseudo-time step:

$$\left(\delta \varepsilon^{VP}\right)^i = \Delta t \left(\xi^{VP}\right)^i; \tag{17}$$

$$\left(\Delta \varepsilon^{VP}\right)^{i} = \left(\Delta \varepsilon^{VP}\right)^{i-1} + \left(\delta \varepsilon^{VP}\right)^{j}.$$
 (18)

Since the time step for unconditional numerical stability is dependent on the stated failure criterion, the Mohr–Coulomb criterion:

$$\Delta t = \frac{4(1+\nu)(1-2\nu)}{E(1-2\nu+\sin^2\varphi)},\tag{19}$$

where v is Poisson's ratio and E is the modulus of elasticity. The derivatives of the potential function (Q) concerning stresses are conveniently expressed through the chain rule; thus:

$$\frac{\partial Q}{\partial \sigma} = \frac{\partial Q}{\partial \sigma_m} \frac{\partial \sigma_m}{\partial \sigma} + \frac{\partial Q}{\partial J_2} \frac{\partial J_2}{\partial \sigma} + \frac{\partial Q}{\partial J_3} \frac{\partial J_3}{\partial \sigma}.$$
 (20)

Summing the following integrals for all elements having a yielding Gauss point, the body loads P_b^l are accumulated at each time step inside each load phase:

$$P_b^i = P_b^{i-1} + \sum_{element}^{all} \int B^T D^e \left(\delta \varepsilon^{VP} \right)^i d(element). \tag{21}$$

At each time step or iteration, this process is repeated until no Gauss point stresses violate the failure condition within a given tolerance. The convergence criterion is based on a dimensionless measure of the change in the displacement increment vector I from iteration to iteration. Description of the entire algorithm are given in [20].

2.3. Factor of Safety Calcualtion

ADONIS is a free geotechnical nonlinear finite element software (http://geowizard.org) that employed the visco-plastic algorithm presented by Smith and Griffiths [20]. The problem to be investigated is a Mohr–Coulomb slope subjected to gravity loading. The FS of the slope must be determined, and this factor is defined as the proportion by which tan (\varnothing) and C must be reduced to induce failure. This differs from the author's software, which caused failure by raising loads while keeping the material attributes constant.

From integrals of the type, the gravity loading vector P_a for material with unit weight (γ) is accumulated for each element.

$$P_{a} = \gamma \sum_{element}^{all} \int N^{T} d\left(element\right). \tag{22}$$

These computations are made in the same program that creates the global stiffness matrix. It is worth noting that the integrals only include the freedoms that correspond to vertical movement. The 1-d array ELD is used at the element level to collect the contributions from each Gauss point. After multiplying by the unit weight GAMA (γ) , the global gravity loads vector GRA VLO gathers ELD from each element.

In this software, the gravity loads vector is applied to the slope in a single increment, and the "load increment loop" is now known as the "trial factor of safety loop". Each step in this loop corresponds to a distinct soil strength parameter's FS. The elastoplastic analysis requires calculated soil strength parameters, which are obtained.

$$\emptyset_f = \arctan(\tan \emptyset/FOS);$$
 (23)

$$C_f = \frac{C}{FOS}. (24)$$

Several (typically increasing) values of the FS are tried until the algorithm fails to converge while keeping the load constant. The value to induce failure is the actual factor of slope safety.

2.4. Slope Stability Analysis

Three slope angle geometries were considered for the analysis (1H:1V), (2H,1V), and (3H:1V) as shown in Figs. 3a, b and c, respectively. Fig. 3 also illustrates the typical generated finite element mesh with the boundary condition of the slope problem. The parametric studies were the slope angle and binder contents in the gypseous soil.

3. Results and Discussion

Table 5 presents the safety factors calculated for the three slopes of gypseous soils stabilized with various percentages of cutback asphalt and lime binders. Results of the slope stability assessment indicated that the gentlest slope of (3H:1V) produced a higher FS compared to the other steeper ones. Such slope geometry impact on the slope stability was also reported by Shiferaw [1] and Taher et al. [24]. By decreasing the slope angles from 1:1 to 3:1, the safety factor increased by a range of 76 % to 84 % for all treated gypseous soils and by about 107 % for the untreated gypseous soil. The optimum percentage of cutback asphalt that produced the highest FS was found to be 6 %. This observation differs from the experimental results, in which 4 % was the optimum content of cutback asphalt. The reason could be related to the fact that the numerical analysis takes into consideration various stress distributions for each point along the failure surface, such as triaxial compression, direct simple shear, and triaxial extension, whereas the experiment results were only based on the direct shear tests [25] as explained in Fig. 4.

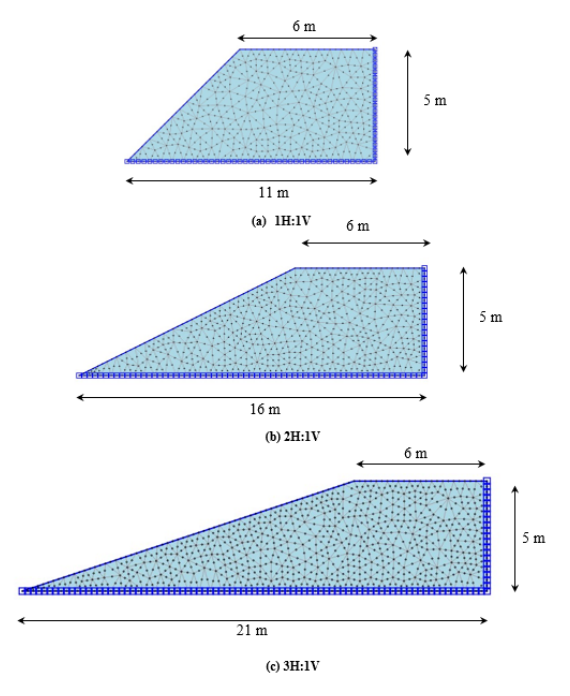


Figure 3. Typical generated mesh for prototype slopes geometry at (a) 1H:1V, (b) 2H:1V and (c) 3H:1V.

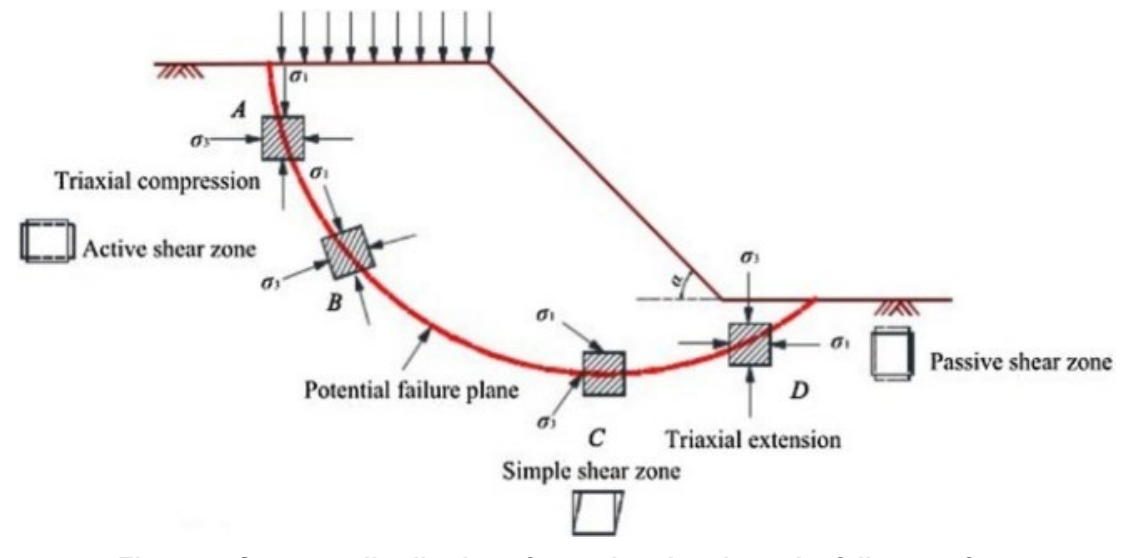


Figure 4. Stresses distributions for each point along the failure surface (after Nitzsche and Herle) [25].

The results presented in Table 5 also revealed that the stability of the slope was further improved when gypseous soils stabilized with mixed binders of 4 % MC and up to 5 % L. While no improvements were obtained with further addition of lime. Thus, it can be concluded that the greatest increase in the degree of stability was observed on slopes of gypseous soil with 4 % MC and 3 % L added binders. The reason could be mainly related to the increase in the soil strength (see Table 4), which resulted in increasing the FS.

Figs. 5a, b and c show the percentage increase in the FS versus the percentage of binders in the gypseous soil for slope angles 1:1, 2:1 and 3:1, respectively. The increasing percentage in the FS was calculated based on the following Equation:

$$FS(increasing\ percentage\ \%) = \frac{FS_{treated\ soil} - FS_{untreated\ soil}}{FS_{untreated\ soil}} \times 100. \tag{25}$$

It can be noticed from the results that the best increase in the FS of about 155 % was produced by the steepest slope followed by 130 % for the slope of 2H:1V and 120 % for the gentlest slope.

Table 5. Factors of the safety of the three slope angles with different percentages of binders.

Diadamana atau	FS		
Binder percentage	1 H:1 V	2 H:1 V	3 H:1 V
0 % MC	2.467	3.838	5.110
2 % MC	3.904	5.580	7.182
4 % MC	5.092	7.221	9.225
6 % MC	5.264	7.373	9.373
8 % MC	4.826	6.787	8.650
10 % MC	4.752	6.678	8.510
4 % MC + 3 % L	6.275	8.873	11.279
4 % MC + 5 % L	6.193	8.686	11.029
4 % MC + 7 % L	4.873	6.721	8.592
4 % MC + 9 % L	4.135	5.783	7.314

Fig. 6 presents the contours of the total displacement of the slope (3H:1V) at three selected percentages of the binder. It can be observed that as the binder content increased, the deformation decreased. The results of the failure mechanism slope also indicated that the majority of the failure surface was circular, which can be classified as face slope failure. This is because the soil employed in this study was gypseous soil, which is prone to collapse at the slope's face.

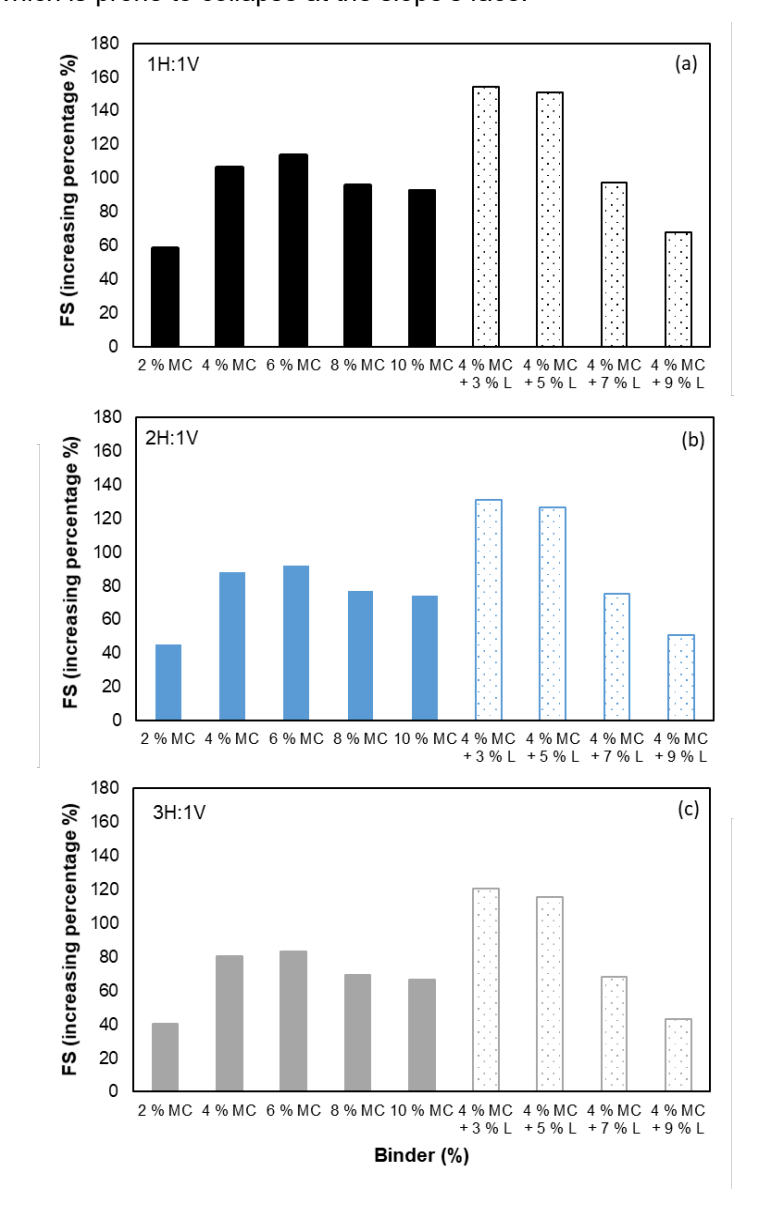


Figure 5. Percentage of increase in the FS with different content of binders of the three slopes at (a) 1H:1V, (b) 2H:1V and (c) 3H:1V.

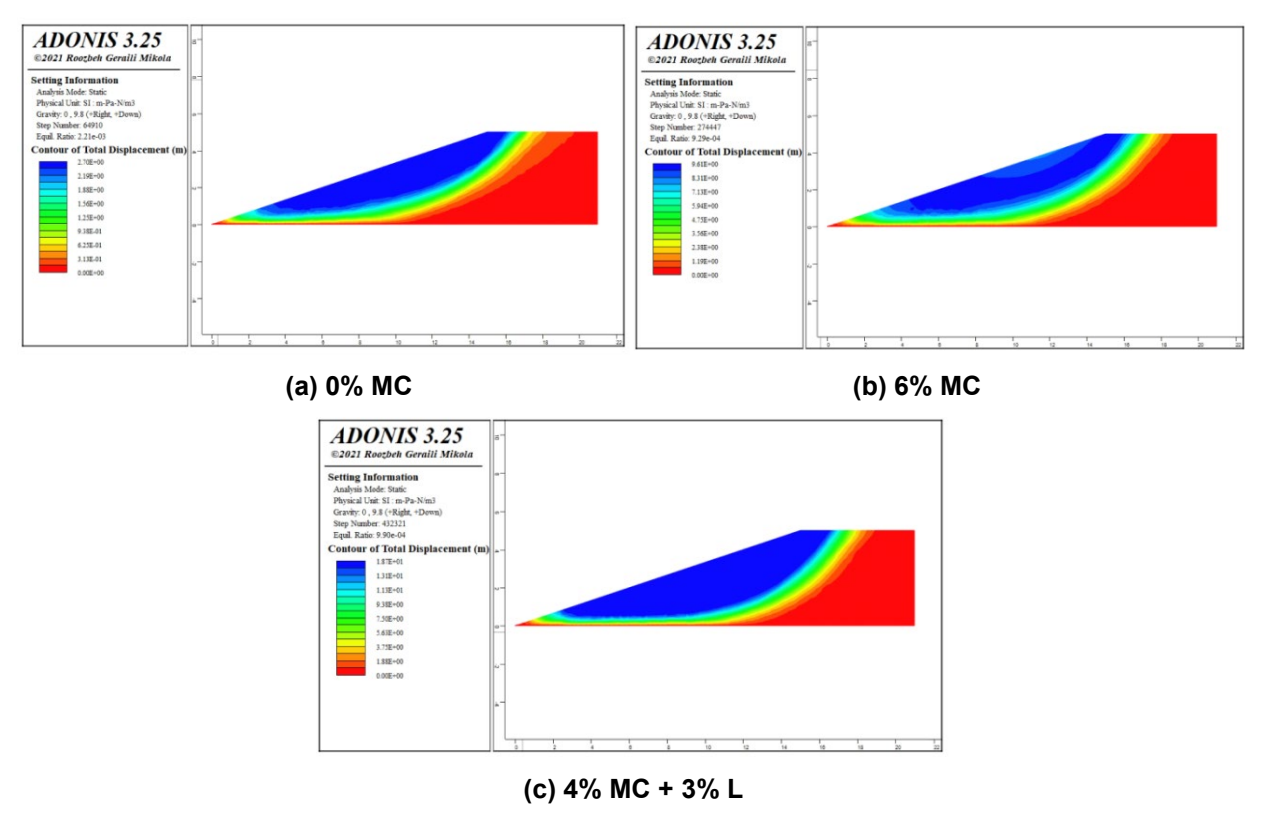


Figure 6. Contours of total displacement of 3H:1V slope at (a) 0% MC, (b) 6% MC and (c) 4% MC + 3% L.

4. Conclusions

The stability of slopes of gypseous soil stabilized with different percentages of cutback asphalt and lime was assessed using ADONIS computer program based on the FEM. The influence of slope angle (H:V) and binder percentages were considered in the analysis. The main findings from the numerical analysis can be summarized as follows: [1]

- 1. The angle of the slope has a substantial impact on slope stability. Such that, when the slope angle was changed from the steepest (1H:1V) to the gentlest (3H:1V), the safety factor increased dramatically. A similar finding was also reported by Shiferaw, and Taher et al. [23].
- 2. Based on the calculated FS, it can be suggested that stabilization of gypseous soil with cutback asphalt and lime offers a possible implication of the improved soil in engineering practice.
- Results of the stability analysis revealed a disagreement with the experimental results concerning
 the optimum content of the cutback asphalt stabilizer. The numerical results showed that when
 stabilizing the gypseous soil with cutback asphalt alone, the 6 % MC provides the highest safety
 factor.
- 4. The greatest stability of slopes was attained when gypseous soils were stabilized using 4 % MC and 3 % L at a slope angle of 3H:1V.
- Comparison between unstabilized and stabilized gypseous soil indicated that the steepest slope of 1H:1V provided the greatest increase in the safety factor.

References

- Shiferaw, H.M. Study on the influence of slope height and angle on the factor of safety and shape of failure of slopes based on strength reduction method of analysis. Beni-Suef University Journal of Basic and Applied Sciences. 2021. 10(1). Article no. 31. DOI: 10.1186/s43088-021-00115-w
- 2. Gör, M., Taher, N., Aksoy, H., Ahmed, H. Effect of Geogrid Inclusion on the Slope Stability. Proceedings of 5th International European Conference on Interdisciplinary Scientific Research. Valencia, 2022. Pp. 275–286.
- Halder, A., Nandi, S., Bandyopadhyay, K. A Comparative Study on Slope Stability Analysis by Different Approaches. Lecture Notes in Civil Engineering. 85. Geotechnical Characterization and Modelling. Spinger. Singapore, 2020. Pp. 285–293. DOI: 10.1007/978-981-15-6086-6_23
- Broms, B., Wong, I. Stabilization of slopes with geofabric. Proceedings of Third International Geotechnical Seminar on Soil Improvement Methods. Singapore, 1985. Pp. 75–83.

- 5. Abd Hacheen, Z. Finite Element Method for Evaluation of Gypseous Soil Treated with Emulsified Asphalt for Sloped Embankment. Engineering and Development Journal. 2008. 12. Pp. 111–128.
- Anvari, S.M., Shooshpasha, I., Kutanaei, S.S. Effect of granulated rubber on shear strength of fine-grained sand. Journal of Rock Mechanics and Geotechnical Engineering. 2017. 9(5). Pp. 936–944. DOI: 10.1016/j.jrmge.2017.03.008
- 7. Li, W., Kwok, C.Y., Senetakis, K. Effects of inclusion of granulated rubber tires on the mechanical behaviour of a compressive sand. Canadian Geotechnical Journal. 2020. 57(5). Pp. 763–769. DOI: 10.1139/cgj-2019-0112
- 8. Aksoy, H.S., Taher, N., Awlla, H. Shear strength parameters of sand-tire chips mixtures. Gümüşhane Üniversitesi Fen Bilimleri Dergisi. 2021. 11 (3). Pp. 713–720. DOI: 10.17714/gumusfenbil.865490
- 9. Barzanji, A.F. Gypsiferous soils of Iraq. PhD Thesis. Civil Engineering Department. Ghent University, 1973.
- 10. Barazanji, K.K.H. Infiltration rate characteristics of gypsiferous soils in Northern Iraq (Jazirah-Area). MSc Thesis. Department of Irrigation and Drainge Engineering. University of Mosul, 1984.
- 11. Woods, K.B. Highway Engineering Handbook. 1st edn. McGraw-Hill Education. NY, 1960. 1665 p.
- 12. Rogers, M., Enright, B. Highway engineering. 3rd edn. Wiley-Blackwell, 2016. 432 pp.
- 13. Guyer, J.P. Introduction to Soil Stabilization in Pavements. Continuing Education and Development, Inc. Woodcliff Lake, NJ, 2011. 29 p.
- Consoli, N.C., Lopes, L.d.S., Prietto, P.D.M., Festugato, L., Cruz, R.C. Variables Controlling Stiffness and Strength of Lime-Stabilized Soils. Journal of Geotechnical and Geoenvironmental Engineering. 2011. 137(6). Pp. 628–632. DOI: 10.1061/(ASCE)GT.1943-5606.0000470
- Haerry, F.A. Lime-Treated Soil Construction Manual: Lime Stabilization and Lime Modification. National Lime Association. 2004. 326(5). Pp. 67–92.
- Thompson, M.R. Lime Reactivity of Illinois Soils. Journal of the Soil Mechanics and Foundations Division. 1966. 92(5). Pp. 67–92.
- 17. Diamond, S., Kinter, E.B. Mechanisms of Soil-Lime Stabilization. Highway Research Record. 1965. 92. Pp. 83–102.
- 18. Archibong, G., Sunday, E., Akudike, J., Okeke, O., Amadi, C. A review of the principles and methods of soil stabilization. International Journal of Advanced Academic Research. Sciences, Technology and Engineering. 2020. 6(3). Pp. 2488–9849.
- 19. Al-Safarani, M. Improvement Ability of Gypseous Soil Characteristics Using Cutback Aasphalt and Lime. MSc Thesis. Civil Engineering Department. Mustansiriyah University, 2007.
- 20. Smith, I.M., Griffiths, D.V., Margetts, L. Programming the Finite Element Method. 5th edn. John Wiley & Sons. NY, 2013. 688 p.
- 21. Yu, H.-S. Plasticity and Geotechnics: Advances in Mechanics and Mathematics. 1st edn. Springer Science & Business Media, 2007. 522 p.
- 22. Reddy, J.N. An Introduction to the Finite Element Method. 3rd ed. McGraw-Hill Education. NY, 2019. 784 p.
- 23. Zienkiewicz, Cecil, O., Morice, P. The Finite Element Method in Engineering Science. 1st edn. McGraw-Hill. London, 1971. 521 p.
- 24. Taher, N.R., Mesut, G., Aksoy, H.S., Ahmed, H. Numerical investigation of the effect of slope angle and height on the stability of a slope composed of sandy soil. Gümüşhane Üniversitesi Fen Bilimleri Dergisi. 2022. 12(2). Pp. 664–675. DOI: 10.17714/gumusfenbil.1051741
- Nitzsche, K., Herle, I. Strain-dependent slope stability. Acta Geotechnica. 2020. 15(11). Pp. 3111–3119. DOI: 10.1007/s11440-020-00971-3

Information about the authors:

Zuhair Abd Hacheem, PhD

E-mail: zuhairabd@uomustansiriyah.edu.iq

Sahar Al-Khyat, PhD

E-mail: saharalkhyat@uomustansiriyah.edu.iq

Khitam Abdulhussein Saeed, PhD

E-mail: khitamhussein@uomustansiriyah.edu.iq

Sabah Fartosy, PhD

ORCID: https://orcid.org/0000-0001-5831-297X E-mail: dr.sabah77@uomustansiriyah.edu.iq

Received 01.02.2023. Approved after reviewing 19.10.2024. Accepted 26.10.2024.